

CrossMark  
click for updatesCite this: *RSC Adv.*, 2014, 4, 37288

# Highly selective catalytic hydrodeoxygenation of $C_{\text{aromatic}}-\text{OH}$ in bio-oil to cycloalkanes on a Ce–Ni–W–B amorphous catalyst

Weiyan Wang,<sup>\*ab</sup> Zhiqiang Qiao,<sup>a</sup> Kun Zhang,<sup>a</sup> Pengli Liu,<sup>a</sup> Yunquan Yang<sup>\*ab</sup> and Kui Wu<sup>a</sup>

This study focused on the preparation of Ce–Ni–W–B amorphous catalysts and the effect of Ce content on their catalytic activities in the hydrodeoxygenation (HDO) of phenols in bio-oil. Adding the promoter Ce could increase the content of  $\text{Ni}^0$  and  $\text{WO}_3$  on the Ce–Ni–W–B catalyst surface, leading to the improvement of the deoxygenation activity, but excess Ce would cover some active sites, resulting in a reduction of the catalytic activity. Because of the amorphous structure and the electron transfer between  $\text{Ni}^0$  and  $\text{B}^0$ , these catalysts possess very high hydrogenation activity, making the HDO of phenols on these amorphous catalysts proceed with a hydrogenation-dehydration route, which not only decreases the aromatic content in the product but also the reaction temperature. With an optimal Ce content (2.5 mol%), the total aromatic selectivity reduced to 1.0% and the HDO reaction temperature decreased to 498 K. This research provides a high activity catalyst for transforming phenols into cycloalkanes.

Received 10th May 2014  
Accepted 11th August 2014

DOI: 10.1039/c4ra04364b

www.rsc.org/advances

## 1. Introduction

Bio-oil, derived from biomass by liquefaction or pyrolysis, has been considered as the most potential replacement or supplement for conventional transportation fuels due to growing energy consumption, the depletion of non-renewable fossil fuel resources and the global greenhouse effect.<sup>1–3</sup> However, this bio-oil contains numerous kinds of oxygenic compounds including phenols, aldehydes and esters, contributing to its high oxygen content, which leads to a poor heating value, thermal instability and tendency of polymerization during storage and transportation.<sup>4,5</sup> Therefore, for a satisfactory result, the oxygen content in bio-oil has to be reduced. Catalytic hydrodeoxygenation (HDO) is deemed to be a particularly effective method to remove the oxygen and increase the H/C atomic ratio of the bio-oil.

Phenols are often selected as the model compounds for the HDO of bio-oil because they account for a large proportion in the bio-oil and the  $C_{\text{aromatic}}-\text{OH}$  bond is stronger than the other C–O bonds.<sup>6,7</sup> Generally, phenols HDO mechanism includes direct hydrogenolysis (DDO) route yielding aromatic products and hydrogenation-dehydration (HYD) route producing cycloalkanes,<sup>8,9</sup> as shown in Fig. 1. Conventional molybdenum

sulfide catalysts promoted by cobalt (Co) or nickel (Ni) were investigated extensively.<sup>9–14</sup> One of the worst inherent disadvantages of these sulfides is the negative effect of oxygen for its sulfidation level.<sup>15,16</sup> Noble metal catalysts possess high hydrogenation activity,<sup>17–20</sup> favoring mild required reaction conditions and a low aromatics content in the final product,<sup>8,21</sup> but the high cost prevents their wide application. Recently, some other catalysts such as transition metal phosphides,<sup>22–25</sup> nitrides<sup>26,27</sup> and metal catalyst<sup>28,29</sup> also show high HDO activity. For these above catalysts, except for some noble metal catalysts, a serious problem worthy to be pointed out is that the HDO reaction temperature is always higher than 573 K,<sup>12,23,28–30</sup> resulting in a high energy consumption and high content of benzene/aromatics in the products. However, aromatics were confirmed to be the environmental carcinogens. If the fuel contained much aromatics such as benzene and its derivatives, there would exhaust some aromatics to the air when this fuel

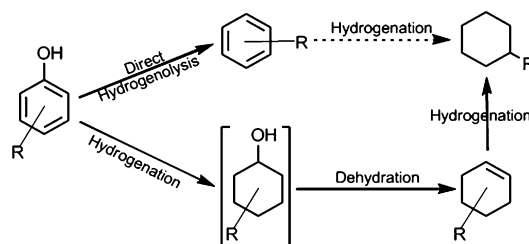


Fig. 1 Reaction network for the HDO of phenols.

<sup>a</sup>School of Chemical Engineering, Xiangtan University, Xiangtan, Hunan, 411105, P. R. China. E-mail: wangweiyang@xtu.edu.cn

<sup>b</sup>National & Local United Engineering Research Center for Chemical Process Simulation and Intensification, Xiangtan University, Xiangtan 411105, P. R. China. E-mail: yangyunquan@xtu.edu.cn

combusted not completely, which would threaten the human health terribly. Hence, the quality standards for clean fuel were become stricter with the increasing demand of environmental protection and World Fuel Oil Regulation IV limited the benzene and aromatics content in gasoline within 1% and 35%, respectively. Therefore, how to develop an innovative HDO catalyst with high activity, non-sulfurization, non-noble metal is still a significant challenge.

Previous studies<sup>8,31–33</sup> had demonstrated that if the catalyst has a high hydrogenation activity to facilitate the HDO of phenols with the route of hydrogenation of the aromatic ring followed by dehydration of the formed alcohols, it would decrease the required HDO temperature, which can realize the energy saving and consumption reduction. Li *et al.* had reported that adding Ce into Ni–B amorphous catalyst could increase its thermal stability, surface area and catalytic activity.<sup>34</sup> We had verified that La-promoted Ni–W–B amorphous catalyst has a high HDO activity, but its thermal stability and Brønsted acid sites needed to be further improved.<sup>31</sup> Therefore, to overcome these shortcomings, in this study, we synthesized a series of Ce promoted Ni–W–B amorphous catalysts and focused on the effect of Ce on their HDO performances using phenol derivatives as the model substrate.

## 2. Experimental section

### 2.1 Catalyst preparation

Ce-promoted Ni–W–B amorphous catalysts were prepared by the following steps: Sodium tungstate (2.94 g), nickel nitrate and cerium nitrate were dissolved in 100 mL aqueous solution, where the Ni/W molar ratio in each case was 1.1 : 1. This mixture solution was placed in a 250 mL three-necked flask. An 80 mL sodium borohydride aqueous solution (1 mol L<sup>-1</sup>) was added dropwise to the three-necked flask with vigorous agitation at 273 K. Then, the black precipitate was produced, which was washed with ultra-pure water several times until the pH = 7 to remove the soluble boron species and Na<sup>+</sup> ions. This was followed by washing with absolute ethanol several times to remove the residual water and water-soluble impurities. Finally, the resulting product was dried under vacuum at 323 K for 8 hours. The resulting material was donated as X Ce where X represented the molar ratio of Ce<sup>3+</sup>/W<sup>6+</sup> in the form of X:1000 in the initial solution. Ni–Mo–S/γ-Al<sub>2</sub>O<sub>3</sub> (γ-Al<sub>2</sub>O<sub>3</sub>, 156.2 m<sup>2</sup> g<sup>-1</sup>) was also prepared for comparison using a mixture of 3.0 wt% carbon disulfide in cyclohexane, as described in the previous literature.<sup>30</sup>

### 2.2 Catalyst characterization

Specific surface area was measured by a Quantachrome's NOVA-2100e Surface Area instrument by physisorption of nitrogen at 77 K. X-ray diffraction (XRD) test was carried out on a D/max 2550 18 KW Rotating anode X-ray Diffractometer with Cu Kα (λ = 1.5418 Å) radiation (40 kV, 300 mA). The 2θ was scanned over the range of 10–80° at a rate of 10° per min to identify the amorphous structure. Bulk compositions were identified by Inductively Coupled Plasma analysts (ICP) on a Varian

VISTAMPX. The surface composition and surface electronic state were analyzed by X-ray Photoelectron Spectroscopy (XPS) using Kratos Axis Ultra DLD instrument at 160 eV pass energy. Al Kα radiation was used to excited photoelectrons. The binding energy value of each element was corrected using C<sub>1s</sub> = 284.6 eV as a reference. The XP spectra of each element was deconvoluted using a Gaussian–Lorentz curve-fitting program. The surface composition of each sample was calculated using the corresponding peak areas of Ni, W, B, Ce and the sensitivity factors for these elements.

### 2.3 Catalyst activity measurement

The catalyst activity tests were carried out in a 300 mL sealed autoclave. The fresh catalyst (0.1 g or 0.3 g), phenols (0.12 mol) and dodecane were placed into the autoclave. The total weight of substrate and dodecane was 100 g. Air in the autoclave was evacuated by pressurization-depressurization cycles with nitrogen and subsequently with hydrogen. The mixture was heated at 10 K min<sup>-1</sup> to the desired temperature, then pressurized with hydrogen to 4.0 MPa and stabilized the stirring speed at 700 rpm. During the reaction, liquid samples were withdrawn from the reactor and identified by Agilent 6890/5973N GC-MS. The amounts of substrate and products were analyzed by Agilent 7890 gas chromatography using a flame ionization detector (FID) with a 30 m AT-5 capillary column. Duplicate or triplicate experiments were performed and the average of these tests is reported here. The errors for conversion values were typically within plus/minus 5.0 mol%. Conversion = (the amount of aromatic-ring change during reaction/total amount of aromatic-ring) × 100%; selectivity = (C atom in each product/total C atom in the products) × 100%; deoxygenation degree (DD, wt%) is defined as [1 – oxygen content in the final organic compounds/total oxygen content in the initial material] × 100%. Carbon balance is better than 96 ± 3% in this work.

## 3. Results and discussion

### 3.1 Characterization of the amorphous catalysts

Fig. 2 shows the XP spectra of the Ni–W–B and Ce–Ni–W–B catalysts in Ni 2p, W 4f, B 1s and Ce 3d levels, respectively. Each of the spectra was deconvoluted, and the relative content of each state was calculated according to the corresponding peak area. Because the elements on catalyst surface were inevitable to be oxidized during synthesis and characterization, peaks for oxidized metal and B species dominated the XPS spectra. The Ni 2p spectra of the Ni–W–B or Ce–Ni–W–B consists of a small peak at 852.5 eV, assigning to metallic nickel (Ni<sup>0</sup>),<sup>35–39</sup> and of three major peaks at higher binding energies (>854.0 eV) to Ni<sup>2+</sup> species.<sup>35–39</sup> Two peaks around 188.0 eV and 192.0 eV are observed in the B 1s spectra, corresponding to B<sup>0</sup> and B<sup>3+</sup>,<sup>39–41</sup> respectively. In comparison with the standard binding energies of pure elemental Ni (853.0 eV) and B (187.1 eV),<sup>39</sup> the binding energy of Ni<sup>0</sup> in the obtained samples shifts negatively by approximately 0.5 eV, whereas the binding energy of B<sup>0</sup> shifts positively by 0.9 eV, suggesting that a partial electron transfers from elemental boron to metallic nickel, which is in agreement

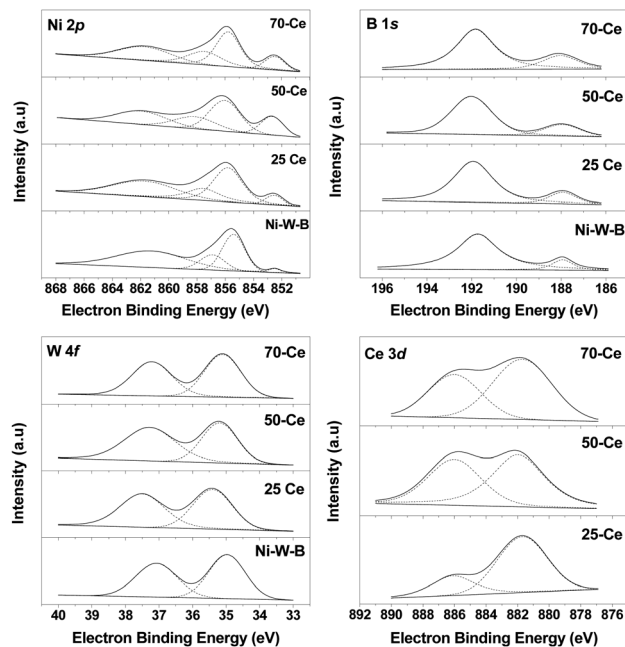


Fig. 2 XPS spectra of Ni 2p, B 1s, W 4f and Ce 3d levels of Ni-W-B and Ce-Ni-W-B samples.

with the previous studies.<sup>35,39–43</sup> This electron transfer, making the Ni<sup>0</sup> electron-enriched and the B<sup>0</sup> electron-deficient, will enhance the hydrogenation activity of the catalyst.<sup>44</sup> Each of the W 4f XPS spectra of these samples is deconvoluted into two peaks at around 35.2 eV and 37.3 eV, corresponding to W 4f<sub>7/2</sub> and W 4f<sub>5/2</sub> doublets of WO<sub>3</sub>,<sup>35,40</sup> respectively, which implies that WO<sub>4</sub><sup>2-</sup> can not be reduced to W<sup>0</sup>. Two peaks at 881.7 eV and 886.1 eV appeared in the Ce 2p XPS spectra are assigned to CeO<sub>2</sub> and Ce<sub>2</sub>O<sub>3</sub>,<sup>34</sup> respectively, indicating that the promoter Ce exists in the form of oxide species in the catalyst. It had reported previously by H. Li *et al.*<sup>34</sup> that Ce oxide species in Ce-Ni-W-B amorphous alloy could act as support. Hence, the presence of Ce oxides in the Ce-Ni-W-B catalysts can prevent the particles from aggregating, which would be significantly improved the surface area and thermal stability of the catalyst.

The bulk composition, surface composition and the content of different valence element of Ce-Ni-W-B are showed in Table 1. Compared with the bulk composition, the Ni/W molar ratio on the surface of Ni-W-B or Ce-Ni-W-B is much higher, indicating that Ni enriches on the catalyst surface. This Ni enrichment might originate from the faster reaction rate of W<sup>6+</sup> with

NaBH<sub>4</sub> than that of Ni<sup>2+</sup> with NaBH<sub>4</sub>. The Ni<sup>0</sup>/Ni<sup>2+</sup> molar ratio for Ni-W-B is 2.9 : 97.1, suggesting that only a minority of nickel presents in a metallic form. The addition of Ce promoter has a great effect for the surface composition. After adding Ce into Ni-W-B, both the W content and B<sup>0</sup> content of the catalyst surface are increased. The Ni<sup>0</sup> content increases from 2.9% for Ni-W-B to 16.9% for 50-Ce, and then decreases to 10.7% for 70-Ce. Although the Ni/W atomic ratio on the catalyst surface decreases with Ce content, it is still much higher than that in bulk composition. The XPS characterization demonstrated that all of W in the prepared catalyst was only existed in the form of WO<sub>3</sub>. According to the reports by X. Li *et al.*<sup>45</sup> that WO<sub>3</sub> in WO<sub>3</sub>/TiO<sub>2</sub> supported catalyst acted as Brønsted acid and the Brønsted acid was inchmeal enhanced with the increase of WO<sub>3</sub> loading. The increase of W content on the catalyst surface means the more Brønsted acid sites.

The bulk composition, surface composition and the content of d As shown in Fig. 3a, fresh Ni-W-B catalyst shows a broad diffraction peak around  $2\theta = 45^\circ$ , characterizing a typical amorphous structure.<sup>35,40,41,44</sup> Other catalysts also present the similar XRD pattern as Ni-W-B, indicating that the addition of Ce promoter does not destroy the amorphous structure. However, the intensity of this peak ( $2\theta = 45^\circ$ ) increases firstly and then decreases with the increase of Ce, suggesting that the amorphous degree of these catalysts are changed, which is mainly caused by the following two reasons. As shown in Table 1, the addition of Ce increases the content of Ni<sup>0</sup> and B<sup>0</sup> on the catalyst surface, enhancing the particle agglomeration because of the strong interaction between Ni<sup>0</sup> and B<sup>0</sup>,<sup>42</sup> which leads to a low amorphous degree. On the other side, Ce oxides in the catalyst, served as a support for the element homogeneous dispersion, hinders the particle agglomeration, which results in a high amorphous degree.<sup>31,34,35</sup> The particle agglomeration leads to produce large particles and then decrease the surface area of sample whereas Ce oxides promote the particle dispersion and then increase its surface area. With these two opposite effects, only a negligible change in the surface area of Ce-Ni-W-B is registered. It is in the order of 50-Ce (47.1 m<sup>2</sup> g<sup>-1</sup>)  $\approx$  25-Ce (47.6 m<sup>2</sup> g<sup>-1</sup>) > Ni-W-B (45.4 m<sup>2</sup> g<sup>-1</sup>) > 70-Ce (35.3 m<sup>2</sup> g<sup>-1</sup>). The low surface area of 70-Ce might be attributed to the insertion of excess Ce oxides in the pore channels of Ni-W-B catalyst.

To further identify the amorphous structure of the prepared catalysts, the fresh catalysts and dodecane were placed into the autoclave and then heat-treated at 523 K or 573 K for 10 h under the condition of 4.0 MPa hydrogen pressure. The corresponding XRD patterns are showed in Fig. 3b and c. The intensity of the

Table 1 Bulk composition and surface composition of Ce-Ni-W-B samples

Catalyst	Bulk composition	Surface composition	Ni (%)		B (%)		W (%)		Ce (%)	
			Ni <sup>0</sup>	Ni <sup>2+</sup>	B <sup>0</sup>	B <sup>3+</sup>	W <sup>0</sup>	W <sup>6+</sup>	Ce <sup>3+</sup>	Ce <sup>4+</sup>
0-Ce	Ni <sub>1.03</sub> W <sub>1.00</sub> B <sub>4.82</sub>	Ni <sub>10.44</sub> W <sub>1.00</sub> B <sub>5.53</sub>	2.9	97.1	11.4	88.6	0	100	—	—
25-Ce	Ce <sub>0.02</sub> Ni <sub>1.01</sub> W <sub>1.00</sub> B <sub>2.34</sub>	Ce <sub>0.02</sub> Ni <sub>4.24</sub> W <sub>1.00</sub> B <sub>2.48</sub>	6.6	94.4	15.6	85.4	0	100	26.8	73.2
50-Ce	Ce <sub>0.05</sub> Ni <sub>1.05</sub> W <sub>1.00</sub> B <sub>1.53</sub>	Ce <sub>0.05</sub> Ni <sub>2.06</sub> W <sub>1.00</sub> B <sub>1.83</sub>	16.9	83.1	20.1	79.9	0	100	43.6	56.4
70-Ce	Ce <sub>0.07</sub> Ni <sub>0.97</sub> W <sub>1.00</sub> B <sub>1.02</sub>	Ce <sub>0.07</sub> Ni <sub>1.95</sub> W <sub>1.00</sub> B <sub>1.21</sub>	10.7	89.3	21.6	78.4	0	100	39.0	61.0

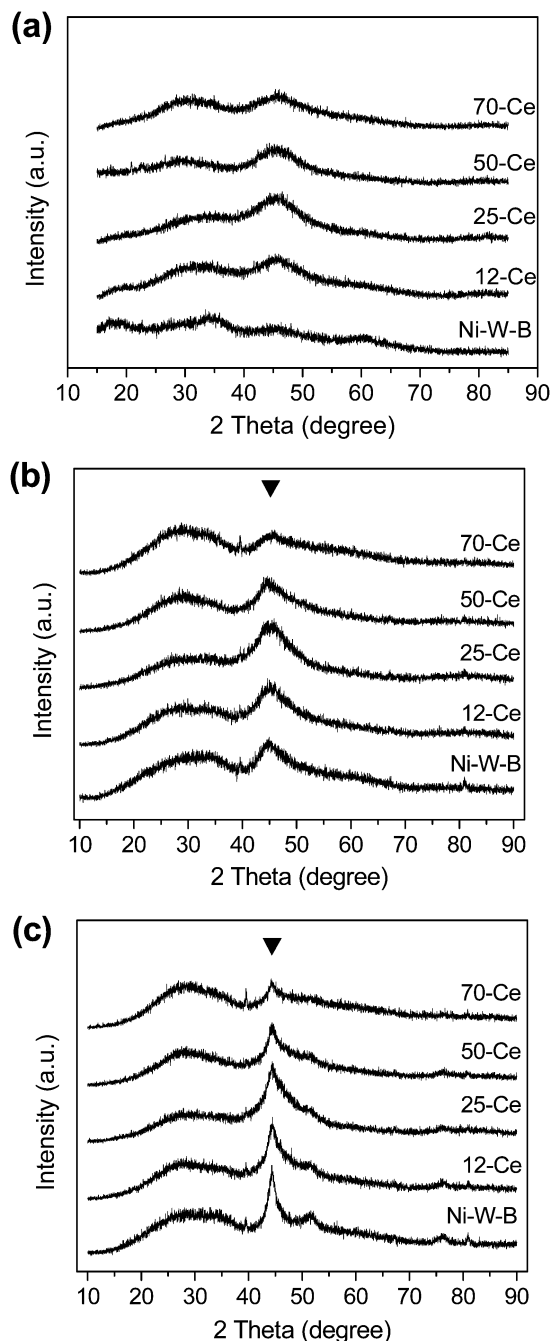


Fig. 3 XRD patterns of Ni-W-B and Ce-Ni-W-B catalysts without heat-treatment (a), heat-treatment at 523 K (b) and 573 K (c).

peak around  $2\theta = 45^\circ$  is gradually strengthened due to a certain level of agglomeration with heat-treated temperature. When heat-treated at 523 K, no obvious diffraction peak can be observed, indicating that the prepared Ce-Ni-W-B catalysts remain the amorphous structure. When the heat-treated temperature is increased to 573 K, Ni-W-B and 12-Ce shows two diffraction peak at  $2\theta = 45^\circ$  and  $52^\circ$ , which corresponds to Ni(111) and Ni(200),<sup>39,46</sup> respectively. This serves as evidence that some metallic Ni had begun to transform from amorphous into crystalline, while the other compounds in Ce-Ni-W-B were

still amorphous in the range of measurement temperature. 25-Ce shows none diffraction peak expect for a very weak and broad one. Fig. 3c also shows that the intensity of the peak around  $2\theta = 45^\circ$  is decreased with the Ce content, suggesting that the thermal stability of Ce-Ni-W-B amorphous catalysts is increased with Ce content, which is consistent with the previous investigation.<sup>34</sup> This positive effect of Ce on the thermal stability is mainly attributed to the support effect of Ce oxides. Ce oxides, acted as support, inhibit the migration of the particles effectively, which is essential for the crystallization. Compared with La-Ni-W-B amorphous catalyst in our previous study,<sup>31</sup> it can conclude that Ce has a better effect for improving the thermal stability of Ni-W-B amorphous catalyst.

### 3.2 Catalyst activity

Generally, the HDO of phenols compounds reacts through two routes: (i) direct C-O bonds scission (DDO) yielding aromatic products and (ii) pre-hydrogenation of the aromatic ring and then dehydration producing cycloalkenes and cycloalkanes (HYD). The *p*-cresol conversion and product selectivity as a function of time in the HDO of *p*-cresol on 25-Ce amorphous catalyst at 498 K are showed in Fig. 4. The *p*-cresol conversion reaches to 99.8% with a selectivity of 82.8% 4-methylcyclohexanol within 1 hour. Then, the HDO of *p*-cresol converts to the HDO of 4-methylcyclohexanol. After 10 hours, the deoxygenation degree reached to 100% with a very little of toluene in the products. This indicates that 25-Ce has a high hydrogenation activity and the deoxygenation reaction is the limited step. For comparison, Ni-Mo-S/ $\gamma$ -Al<sub>2</sub>O<sub>3</sub>, as traditional and industrial catalyst, was also selected as catalyst for the HDO of *p*-cresol. As shown in Fig. 5, no any oxygen-containing compound is found in the products and the 4-methylcyclohexene selectivity is very low during the whole process. After reacting at 573 K for 10 hours, *p*-cresol conversion is only 47.1% with a selectivity of 58.3% methylcyclohexane, whereas the selectivity of toluene obtained by the direct deoxygenation route reaches to 39.4%, indicating that this sulfide catalyst has low hydrogenation but high dehydration at 573 K. According to the above results, it can

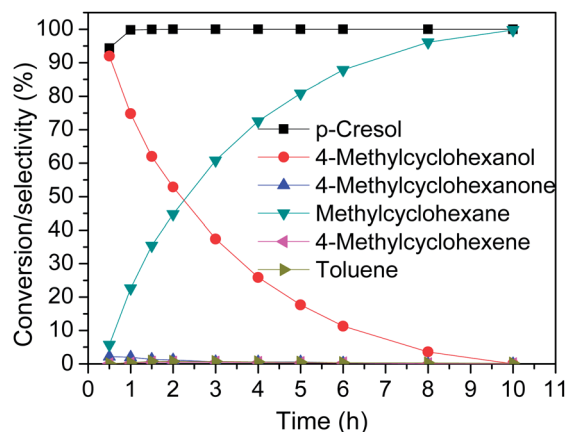


Fig. 4 *p*-Cresol conversion and the product selectivity versus time on 25-Ce. Reaction conditions: 0.10 g catalyst, temperature 498 K.

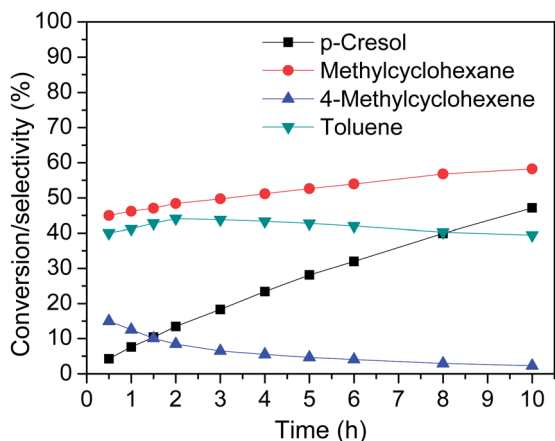


Fig. 5 *p*-Cresol conversion and the product selectivity versus time on Ni–Mo–S/γ–Al<sub>2</sub>O<sub>3</sub>. Reaction conditions: 0.60 g catalyst, temperature 573 K.

be concluded that the dominant route for *p*-cresol HDO on Ce–Ni–W–B is HYD. That was, *p*-cresol is hydrogenated to 4-methylcyclohexanol firstly and then dehydrated. The energy barrier for phenolic hydroxyl is much higher than that for aliphatic hydroxyl. Thus, for the HDO of *p*-cresol, HYD route can not only decrease the reaction temperature but aromatic content in the product.

As shown in Fig. 4, the high conversion and high 4-methylcyclohexanol selectivity within 1 hour indicates a high hydrogenation activity but a low deoxygenation activity for 25-Ce amorphous catalyst. The high hydrogenation activity is attributed to the amorphous structure and electron transfer between Ni<sup>0</sup> and B<sup>0</sup> that facilitated the adsorption of hydrogen on the Ni metal sites with higher electron density to form H<sup>–</sup> species and thus enhanced its hydrogenation activity.<sup>35,42</sup> For Ce–Ni–W–B catalysts, WO<sub>3</sub> on the surface acts as Brønsted acid site. The dehydration of 4-methylcyclohexanol occurs on these Brønsted acid sites, and the deoxygenation rate depends on the number of Brønsted acid site. Compared the hydrogenation activity with the deoxygenation activity, it can conclude that the available Brønsted acid sites for deoxygenation are not enough while the hydrogenation active sites are saturated. This indicates that the matching of Ni metal sites and WO<sub>3</sub> Brønsted acid sites might be unsuitable and the presence of more WO<sub>3</sub> active sites would favor the high deoxygenation degree. To verify this deduction, the effect of catalyst amount for the HDO of *p*-cresol was studied by adding 3 fold amounts of 25-Ce catalyst. As a result, the deoxygenation degree increases from 17.8% (calculated from Fig. 5) to 98.1% (in Table 2), which demonstrates that Brønsted acid sites on Ce–Ni–W–B amorphous catalyst surface needs to be improved. In addition, the catalyst surface enriches with Ni, but only metal Ni possesses the high hydrogenation activity. Therefore, the HDO activity of Ce–Ni–W–B amorphous catalyst can be further enhanced by increasing the metal Ni<sup>0</sup> and WO<sub>3</sub> sites or regulating the matching between these two site types.

The effect of the Ce content for the catalytic activity of Ce–Ni–W–B in the HDO of *p*-cresol is presented in Table 2. The

Table 2 Comparison of Ni–Mo–S/γ–Al<sub>2</sub>O<sub>3</sub> and Ce–Ni–W–B amorphous catalysts with different Ce content in the HDO of *p*-cresol<sup>a</sup>

Catalysts	S <sup>b</sup>	Ni–W–B	12-Ce	25-Ce	50-Ce	70-Ce
Conversion, mol%	47.1	100	100	99.7	99.1	97.7
Products distribution, mol%						
4-Methylcyclohexanol	0	64.6	57.8	1.4	3.4	5.5
3-Methylcyclohexene	2.3	0.9	0.2	0.2	0.2	5.6
Methylcyclohexane	58.3	33.9	41.3	97.4	94.9	78.9
Toluene	39.4	0.6	0.7	1.0	1.5	10.0
DD, wt%	44.1	35.6	41.8	98.1	95.3	91.6

<sup>a</sup> Reaction conditions: 0.30 g catalyst, 12.74 g *p*-cresol, 87.26 g dodecane, temperature 498 K, time 1 h. <sup>b</sup> Reaction conditions: 0.60 g Ni–Mo–S/γ–Al<sub>2</sub>O<sub>3</sub> catalyst, 12.74 g *p*-cresol, 87.26 g dodecane, temperature 573 K, time 10 h.

end products are 4-methylcyclohexanol, 4-methylcyclohexene, methylcyclohexane and toluene. Ni–W–B exhibits a high conversion (100%) but a low deoxygenation degree (35.6%) at 498 K. After adding promoter Ce to Ni–W–B, the deoxygenation activity of the catalyst and the product distribution are significantly changed. The deoxygenation degree of Ce–Ni–W–B is decreased with the order of 25-Ce (98.1%) > 50-Ce (95.3%) > 70-Ce (91.6%) > 12-Ce (41.8%) > Ni–W–B (35.6%) and the selectivity of 4-methylcyclohexanol presents an opposite trend. The deoxygenation degree reaches to 98.1% and the selectivity of 4-methylcyclohexanol decreases to 1.4% on 25-Ce at 498 K for 1 hour, showing that the Ce–Ni–W–B amorphous catalyst has much higher HDO activity than the previous catalysts.<sup>22,30,33</sup>

For the HDO on Ce–Ni–W–B amorphous catalysts, the main reaction route is HYD (*p*-cresol → 4-methylcyclohexanol → 3-methylcyclohexene → methylcyclohexane). Under the studied reaction conditions, the high conversion of *p*-cresol on Ni–W–B and Ce–Ni–W–B catalysts is mainly attributed to the unique amorphous structure and the electronic interaction between metallic Ni and the elemental B. The addition of Ce promoter leads to produce more metallic Ni than that without any promoter. This metallic Ni is electron-enriched, which could increase the back donation of electrons to the π\* (anti-bonding) of aromatic ring in chemisorbed phenol, making the aromatic ring activated towards hydrogenation.<sup>47</sup> However, in this study, the end aim is a high deoxygenation degree but not a high conversion, and the deoxygenation is usually occurred on Brønsted acid sites. When adding Ce promoter, WO<sub>3</sub>, acted as Brønsted acid site, was increased, leading to the high deoxygenation degree. But, high Ce amount is harmful for the activity. As shown in Table 2, the *p*-cresol conversion is gradually decreases from 99.7% for 25-Ce to 97.7% for 70-Ce and the deoxygenation degree is decreased from 98.1% for 25-Ce to 91.6% for 70-Ce. The XPS characterization results showed that Ce was existed in the form of oxides, which is inactive for the hydrogenation. On the other hand, excess Ce oxides blocked the pore channels of Ni–W–B, leading to a low surface area and low amount of available active sites. Hence, the reduction in conversion and deoxygenation degree on 70-Ce is resulted from the coverage of surface active sites by Ce oxides and the decrease of surface area.

According to World Fuel Oil Regulation, the less the aromatic content is the better. For the HDO of *p*-cresol, the products (methylcyclohexane and toluene) distribution depends on the molecular adsorption modes on the catalyst surface. Vertical orientation that *p*-cresol is adsorbed on the catalyst *via* the hydroxyl group facilitates the removal of oxygen to form toluene while coplanar adsorption that aromatic ring adsorbed on the catalyst followed saturating to yield 4-methylcyclohexanol as an intermediate.<sup>48</sup> Table 2 shows the toluene selectivity is increased from 0.6% on Ni–W–B to 10.0% on 70–Ce, indicating that the vertical orientation adsorption is enhanced. This change accounting for effect of Ce content can be attributed to Ce(III) species. Ce(III) species in Ce–Ni–W–B amorphous catalysts enhances the hydrophilicity of the catalysts, which is beneficial to accept the lone electron pair on the oxygen atom from phenolic hydroxyl.<sup>49</sup> That is, Ce(III) species adsorb *p*-cresol *via* vertical orientation mode. Therefore, the higher the content of Ce was in the catalyst surface, the more the Ce(III) species was, and then the higher is toluene selectivity.

Fig. 6 shows the recycling tests using 25–Ce catalyst at 498 K. the conversion was decreased while both 3-methylcyclohexene selectivity and toluene selectivity were increased with the increase of recycling numbers. This suggested that the hydrogenation activity of 25–Ce was declining. After five recycle reactions, the structure of 25–Ce catalyst was characterized by XRD, as shown in Fig. 7. Compared with fresh catalyst, three peak were observed at  $2\theta = 45^\circ$ ,  $52^\circ$  and  $76^\circ$  in the XRD pattern of 25–Ce catalyst after reaction, corresponding to Ni(111), Ni(200) and Ni(220),<sup>46</sup> but these peaks were not very sharp, which indicated that only partial amorphous Ni was transformed to crystalline Ni. This transformation made the hydrogenation activity of the catalyst reduced,<sup>44,50</sup> which can be prevented efficiently by preparing supported catalyst.

Based on the excellent performance of 25–Ce in the HDO of *p*-cresol, the generality of this catalyst was investigated through a series of phenol derivatives. The results are summarized in Table 3. All the phenols evaluated in this study, except for methoxyl substituted phenols, are efficiently converted to the

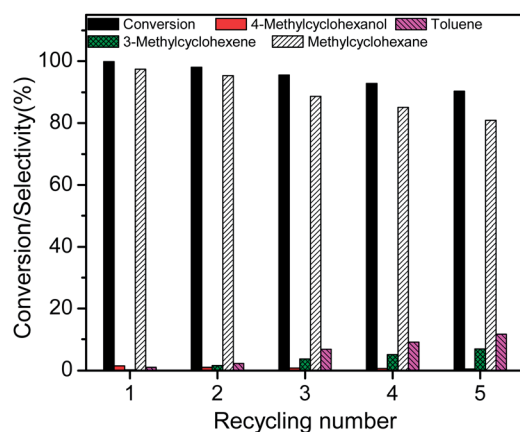


Fig. 6 Recycling tests of 25–Ce for the HDO of *p*-cresol. Reaction conditions: 0.3 g catalyst, 12.74 g *p*-cresol, 87.26 g dodecane, temperature, 1 h reaction time.

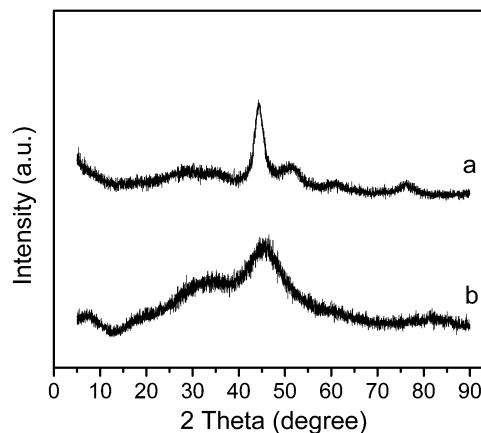


Fig. 7 XRD patterns of 25–Ce catalyst after reaction (a) and before reaction (b).

corresponding cycloalkanes in selectivity no less than 98.0%. The product mixtures include very low concentrations of benzene/aromatics. For the methoxyl substituted phenols, the methoxyl group was hydrolyzed to give small molecules such as methanol and methane, leading to a selectivity of 85% cycloalkanes. Notably, when the conversion reaches to nearly 100%, the reaction time for *m*-substituted and *p*-substituted phenols was shorter than that for *o*-substituted phenols. In fact, phenols are adsorbed preferentially *via* the C–O bond, adjacent groups will interfere this process, causing the difference in the conversion. The above results therefore indicate that Ce–Ni–W–B amorphous catalyst system is applicable to the HDO of various phenol derivatives into cycloalkanes.

Table 3 HDO of phenol derivatives on 25–Ce<sup>a</sup>

Run	Substrate	Time (h)	Conversion (%)	Selectivity (%)
1		1.0	100	100
2		1.5	100	98.9
3		1.0	100	98.6
4		1.5	98.2	98.5
5		2.0	100	100
6		4.0	94.5	100
7		2.0	100	85.2
8		6.0	100	85.0
9		2.0	99.5	99.5

<sup>a</sup> Reaction conditions: 0.30 g catalyst, 0.12 mol substrate, the weight of substrate and dodecane was 100 g, temperature 498 K.

Compared with the sulphide catalysts and metal phosphides in other studies,<sup>12,22,51</sup> the HDO temperature of *p*-cresol on these Ce–Ni–W–B amorphous catalyst is much lower. Since sulphide catalysts and metal phosphides have a low hydrogenation activity, the hydrogenation of *p*-cresol on these catalysts into 4-methylcyclohexanol is hard, not to mention this hydrogenation at a low temperature. On the other hand, the oxygen removed from the phenolic hydroxyl group is much harder than that from the alcoholic hydroxyl group because of its higher energy barrier. If it wants to reach the goal of high deoxygenation degree on sulphides and metal phosphides catalysts, the reaction temperature must be increased. But the direct C–O bonds scission (DDO route) yielding aromatic is easy to occur at high temperature, leading to high aromatic selectivity. In contrast, noble metal Pt possesses a high hydrogenation activity, adopting it as a catalyst for the HDO of phenols can make the HDO reaction proceeded with the hydrogenation-dehydration route, leading to a low aromatics selectivity and reaction temperature.<sup>8,33</sup> Ni based amorphous catalyst, possessing the same or ever higher hydrogenation activity as noble metal Pt catalyst, is widely applied into the hydrogenation.<sup>35–39</sup> In this case, we select amorphous metal Ni and WO<sub>3</sub> as active sites to prepare Ni–W–B catalyst and add promoter Ce to further increase its HDO activity. The metal Ni content and WO<sub>3</sub> are increased by adding Ce promoter, suggesting the more hydrogenation active and deoxygenation sites. *p*-Cresol on these Ce–Ni–W–B amorphous catalysts can be quickly hydrogenated into 4-methylcyclohexanol at low temperature and then deoxygenated on Brønsted acid sites. Both the aromatics content in the products and the HDO temperature are significantly decreased, which decreases the energy consumption for the phenols refining ultimately.

## 4. Conclusions

Ce–Ni–W–B amorphous catalysts were prepared by the chemical reduction method and showed a high catalytic activity for the HDO of phenols in the bio-oil. The effect of promoter Ce on Ni–W–B amorphous catalyst is attributed to the increase of Ni<sup>0</sup> content and WO<sub>3</sub> active sites on catalyst surface and the improvement of thermal stability. With an optimum content of the Ce promoter in the Ni–W–B amorphous catalyst (2.5% mol), the deoxygenation degree is up to 98.1% with a low selectivity of 1.0% toluene in the HDO of *p*-cresol under the conditions of temperature 498 K, hydrogen pressure 4.0 MPa and time 1 hour. Too much Ce will cover some active sites, leading to a decrease of activity and a high content of toluene. The HDO of C<sub>aromatic</sub>–OH on these amorphous catalysts mainly proceeds with hydrogenation-dehydration route. Both the aromatics content in the product and the HDO reaction temperature are decreased obviously, which realizes the energy saving and consumption reduction in the HDO process and displays a tremendous development potential.

## Acknowledgements

This work was supported by the National Natural Science Foundation of China (no. 21306159, 21376202), Specialized

research Fund for the Doctoral Program of Higher Education (20124301120009) and Natural Science Foundation of Hunan Province (13JJ4048).

## Notes and references

- J. Q. Bond, D. M. Alonso, D. Wang, R. M. West and J. A. Dumesic, *Science*, 2010, **327**, 1110–1114.
- T. P. Vispute, H. Zhang, A. Sanna, R. Xiao and G. W. Huber, *Science*, 2010, **330**, 1222–1227.
- F. Shi, P. Wang, Y. Duan, D. Link and B. Morreale, *RSC Adv.*, 2012, **2**, 9727–9747.
- S. Crossley, J. Faria, M. Shen and D. E. Resasco, *Science*, 2010, **327**, 68–72.
- J. Zakzeski, P. C. A. Bruijninx, A. L. Jongerius and B. M. Weckhuysen, *Chem. Rev.*, 2010, **110**, 3552–3599.
- Q. Bu, H. Lei, S. Ren, L. Wang, J. Holladay, Q. Zhang, J. Tang and R. Ruan, *Bioresour. Technol.*, 2011, **102**, 7004–7007.
- H. Wang, J. Male and Y. Wang, *ACS Catal.*, 2013, 1047–1070.
- C. Zhao, Y. Kou, A. A. Lemonidou, X. Li and J. A. Lercher, *Angew. Chem., Int. Ed.*, 2009, **48**, 3987–3990.
- O. I. Şenol, E. M. Ryymin, T. R. Viljava and A. O. I. Krause, *J. Mol. Catal. A: Chem.*, 2007, **277**, 107–112.
- B. Yoosuk, D. Tumnantong and P. Prasassarakich, *Chem. Eng. Sci.*, 2012, **79**, 1–7.
- C. Dupont, R. Lemeur, A. Daudin and P. Raybaud, *J. Catal.*, 2011, **279**, 276–286.
- Y. Q. Yang, C. T. Tye and K. J. Smith, *Catal. Commun.*, 2008, **9**, 1364–1368.
- C. Wang, D. Wang, Z. Wu, Z. Wang, C. Tang and P. Zhou, *Appl. Catal., A*, 2014, **476**, 61–67.
- A. Popov, E. Kondratieva, L. Mariey, J. M. Goupil, J. El Fallah, J.-P. Gilson, A. Travert and F. Maugé, *J. Catal.*, 2013, **297**, 176–186.
- O. I. Şenol, T. R. Viljava and A. O. I. Krause, *Appl. Catal., A*, 2007, **326**, 236–244.
- A. Y. Bunch and U. S. Ozkan, *J. Catal.*, 2002, **206**, 177–187.
- C. Zhao and J. A. Lercher, *ChemCatChem*, 2012, **4**, 64–68.
- H. Ohta, H. Kobayashi, K. Hara and A. Fukuoka, *Chem. Commun.*, 2011, **47**, 12209–12211.
- J. Chen, J. Huang, L. Chen, L. Ma, T. Wang and U. I. Zakai, *ChemCatChem*, 2013, **5**, 1598–1605.
- J. He, C. Zhao and J. A. Lercher, *J. Catal.*, 2014, **309**, 362–375.
- P. T. M. Do, A. J. Foster, J. Chen and R. F. Lobo, *Green Chem.*, 2012, **14**, 1388–1397.
- V. M. L. Whiffen, K. J. Smith and S. K. Straus, *Appl. Catal., A*, 2012, **419–420**, 111–125.
- Y. Yang, A. Gilbert and C. Xu, *Appl. Catal., A*, 2009, **360**, 242–249.
- J.-S. Moon, E.-G. Kim and Y.-K. Lee, *J. Catal.*, 2014, **311**, 144–152.
- W. Wang, K. Zhang, H. Liu, Z. Qiao, Y. Yang and K. Ren, *Catal. Commun.*, 2013, **41**, 41–46.
- I. T. Ghampson, C. Sepúlveda, R. Garcia, B. G. Frederick, M. C. Wheeler, N. Escalona and W. J. DeSisto, *Appl. Catal., A*, 2012, **413–414**, 78–84.

- 27 S. Boulloussa-Eiras, R. Lødeng, H. Bergem, M. Stöcker, L. Hannevold and E. A. Blekkan, *Catal. Today*, 2014, **223**, 44–53.
- 28 R. N. Olcese, M. Bettahar, D. Petitjean, B. Malaman, F. Giovannella and A. Dufour, *Appl. Catal., B*, 2012, **115–116**, 63–73.
- 29 M. V. Bykova, D. Y. Ermakov, V. V. Kaichev, O. A. Bulavchenko, A. A. Saraev, M. Y. Lebedev and V. A. Yakovlev, *Appl. Catal., B*, 2012, **113–114**, 296–307.
- 30 Y. Romero, F. Richard and S. Brunet, *Appl. Catal., B*, 2010, **98**, 213–223.
- 31 W. Wang, Y. Yang, H. Luo, H. Peng and F. Wang, *Ind. Eng. Chem. Res.*, 2011, **50**, 10936–10942.
- 32 W. Y. Wang, Y. Q. Yang, J. G. Bao and H. A. Luo, *Catal. Commun.*, 2009, **11**, 100–105.
- 33 P. T. M. Do, A. J. Foster, J. Chen and R. F. Lobo, *Green Chem.*, 2012, **14**, 1388–1397.
- 34 H. Li, S. Zhang and H. Luo, *Mater. Lett.*, 2004, **58**, 2741–2746.
- 35 B. Zhao, C. J. Chou and Y. W. Chen, *Ind. Eng. Chem. Res.*, 2010, **49**, 1669–1676.
- 36 H. Li, D. Zhang, G. Li, Y. Xu, Y. Lu and H. Li, *Chem. Commun.*, 2010, **46**, 791–793.
- 37 M. H. Lin, B. Zhao and Y. W. Chen, *Ind. Eng. Chem. Res.*, 2009, **48**, 7037–7043.
- 38 P. Kukula, V. Gabova, K. Koprivova and P. Trtik, *Catal. Today*, 2007, **121**, 27–38.
- 39 H. Li, H. Li and J. Deng, *Catal. Today*, 2002, **74**, 53–63.
- 40 N. Patel, R. Fernandes and A. Miotello, *J. Catal.*, 2010, **271**, 315–324.
- 41 G. L. Parks, M. L. Pease, A. W. Burns, K. A. Layman, M. E. Bussell, X. Wang, J. Hanson and J. A. Rodriguez, *J. Catal.*, 2007, **246**, 277–292.
- 42 H. Li, Q. Zhao and H. Li, *J. Mol. Catal. A: Chem.*, 2008, **285**, 29–35.
- 43 Z. Wu, M. Zhang, S. Ge, Z. Zhang, W. Li and K. Tao, *J. Mater. Chem.*, 2005, **15**, 4928–4933.
- 44 H. Li, J. Liu, S. Xie, M. Qiao, W. Dai and H. Li, *J. Catal.*, 2008, **259**, 104–110.
- 45 G. Lu, X. Li, Z. Qu, Q. Zhao, H. Li, Y. Shen and G. Chen, *Chem. Eng. J.*, 2010, **159**, 242–246.
- 46 L. Lu, Z. Rong, W. Du, S. Ma and S. Hu, *ChemCatChem*, 2009, **1**, 369–371.
- 47 H. Li, J. Liu and H. Li, *Mater. Lett.*, 2008, **62**, 297–300.
- 48 H. Wan, R. Chaudhari and B. Subramaniam, *Top. Catal.*, 2012, **55**, 129–139.
- 49 J.-L. Liu, L.-J. Zhu, Y. Pei, J.-H. Zhuang, H. Li, H.-X. Li, M.-H. Qiao and K.-N. Fan, *Appl. Catal., A*, 2009, **353**, 282–287.
- 50 H. Li, H. Li, J. Zhang, W. Dai and M. Qiao, *J. Catal.*, 2007, **246**, 301–307.
- 51 V. M. L. Whiffen and K. J. Smith, *Energy Fuels*, 2010, **24**, 4728–4737.